

MLCM: Multistep Consistency Distillation of Latent Diffusion Model

Qingsong Xie*
OPPO AI Center
xieqingsong1@oppo.com

Zhenyi Liao
Shanghai Jiao Tong University
l-justice@sjtu.edu.cn

Chen Chen
OPPO AI Center
chenchen4@oppo.com

Zhijie Deng*
Shanghai Jiao Tong University
zhijied@sjtu.edu.cn

Shixiang Tang
Chinese University of Hong Kong
shixiangtang@cuhk.edu.cn

Haonan Lu
OPPO AI Center
luhaonan@oppo.com



Figure 1: 1024×1024 image samples from MLCM, distilled from SDXL-base-1.0 [32] based on LoRA [8]. From top to bottom, 2, 3, and 4 sampling steps are adopted, respectively. Apart from such good visual quality, MLCM can also yield improved metrics compared to strong baselines.

Abstract

Distilling large latent diffusion models (LDMs) into ones that are fast to sample from is attracting growing research interest. However, the majority of existing methods face a dilemma where they either (i) depend on multiple individual distilled models for different sampling budgets, or (ii) sacrifice generation quality with limited (e.g., 2-4) and/or moderate (e.g., 5-8) sampling steps. To address these, we extend the recent multistep consistency distillation (MCD) strategy

*Corresponding author.

to representative LDMs, establishing the Multistep Latent Consistency Models (MLCMs) approach for low-cost high-quality image synthesis. MLCM serves as a unified model for various sampling steps due to the promise of MCD. We further augment MCD with a progressive training strategy to strengthen inter-segment consistency to boost the quality of few-step generations. We take the states from the sampling trajectories of the teacher model as training data for MLCMs to lift the requirements for high-quality training datasets and to bridge the gap between the training and inference of the distilled model. MLCM is compatible with preference learning strategies for further improvement of visual quality and aesthetic appeal. Empirically, MLCM can generate high-quality, delightful images with only 2-8 sampling steps. On the MSCOCO-2017 5K benchmark, MLCM distilled from SDXL gets a CLIP Score of 33.30, Aesthetic Score of 6.19, and Image Reward of 1.20 with only 4 steps, substantially surpassing 4-step LCM [23], 8-step SDXL-Lightning [17], and 8-step HyperSD [33]. We also demonstrate the versatility of MLCMs in applications including controllable generation, image style transfer, and Chinese-to-image generation.

1 Introduction

Diffusion models (DMs) have made great advancements in the field of generative modeling, becoming the go-to approach for image, video, and audio generation [6, 14, 35]. Latent diffusion models (LDMs) further enhance DMs by operating in the latent image space, pushing the limit of high-resolution image and video synthesis [27, 31, 32, 34]. Despite the high-quality and realistic samples, LDMs suffer from frustratingly slow inference—generating a single sample requires multiple (from tens to hundreds) evaluations of the model, giving rise to a high cost and bad user experience.

There is growing interest in distilling large-scale LDMs into more efficient ones. Concretely, progressive distillation [17, 28, 36] reduces the sampling steps by half in each turn but finally hinges on a set of models for various sampling steps. InstaFlow [20], UFO-Gen [53], and ADD [37, 38] target one-step generation, yet losing or weakening the ability to benefit from more (e.g., > 4) sampling steps. Latent consistency models (LCMs) [23] apply consistency distillation [45] on LDMs’ reverse-time ordinary differential equation (ODE) trajectories to conjoin one- and multi-step generation, but the image quality degrades substantially, especially in 1-4 steps. HyperSD [33] applies consistency trajectory distillation [10] in segments of the ODE trajectory, but its performance gain is marginal as sampling steps increase and it requires numerous high-quality text-image pairs for training.

To address these, we extend the multistep consistency distillation (MCD) [4] strategy to representative LDMs, forming Multistep Latent Consistency Models (MLCMs) for low-cost high-quality image synthesis. Technically, we divide the latent-space ODE trajectory into multiple segments and enforce consistency within each. MLCM serves as a unified model for various sampling steps without suffering from accumulated errors as in LCM. To further improve the quality of few-step generations, we enhance MLCMs with a progressive training strategy for inter-segment consistency.

Considering the discrepancy between the training and inference of typical LDMs like SDXL [32], where the final state of the forward process is not a pure Gaussian noise [38], we suggest leveraging the states of the denoising process of the teacher model as MLCMs’ training data. Apart from facilitating the alignment between the training and inference, this also helps alleviate the need for high-quality training datasets as in HyperSD. Besides, reward scorers, e.g., Image Reward (IR) [52] and aesthetic score (AS) [39], can be easily incorporated into MLCMs to improve the human preference of the outcomes, thanks to the few-step generation capacity of MLCMs.

We have performed comprehensive empirical studies to inspect the behavior of MLCMs. We first empirically evaluate the image quality on the MSCOCO-2017 5K benchmark. We observe that MLCM distilled from SDXL [32] gets 6.19 AS, 1.20 IR, 33.30 CLIP Score (CS) [5], and 0.233 Pick Score (PS) [12] with only 4 steps, substantially surpassing 4-step LCM, 8-step SDXL-Lightning [17], and 8-step HyperSD. Additionally, the performance of MLCMs consistently improves with additional sampling steps. We also demonstrate the versatility of MLCMs in applications including controllable generation, image stylization, and Chinese-to-image generation.

We summarize our contributions as follows:

- We propose MLCMs, which accelerate LDMs to generate high-quality outputs within 2 – 8 steps while maintaining the capability for further improvement with additional steps.
- We improve MLCMs with a progressive training strategy for inter-segment consistency, render MLCMs image-free during training by exploiting the denoising process of the teacher model, and incorporate preference learning to boost rare-step generation quality.
- MLCM achieves a state-of-the-art CS of 33.30, AS of 6.19, IR of 1.20 in 4 steps, surpassing competing baselines, such as 4-step LCM, 8-step SDXL-Lightning, and 8-step HyperSD.
- MLCMs’ versatility extends to scenarios such as controllable generation, image stylization, and Chinese-to-image generation, paving the path for extensive practical applications.

2 Preliminary

2.1 Diffusion Models

Diffusion models (DMs) [6, 41, 48] are specified by a predefined forward process that progressively distorts the clean data x_0 into a pure Gaussian noise with a Gaussian transition kernel. It is shown that such a process can be described by the following stochastic differential equation (SDE) [9, 48]:

$$dx_t = f(x, t)x_t dt + g(t)dw_t, \quad (1)$$

where $t \in [0, T]$, w_t is the standard Brownian motion, and $f(x, t)$ and $g(t)$ are the drift and diffusion coefficients respectively. Let $p_t(x_t)$ denote the corresponding marginal distribution of x_t .

It has been proven that this forward SDE possesses the identical marginal distribution as the following probability flow (PF) ordinary differential equation (ODE) [48]:

$$dx_t = \left[f(x, t)x_t - \frac{1}{2}g^2(t)\nabla x_t \log p_t(x_t) \right] dt. \quad (2)$$

As long as we can learn a neural model $\epsilon_\theta(x_t, t)$ for estimating the ground-truth score $\nabla x_t \log p_t(x_t)$, we can then draw samples that roughly follow the same distribution as the clean data by solving the diffusion ODE. In practice, the learning of $\epsilon_\theta(x_t, t)$ usually boils down to score matching [48].

The ODE formulation is appreciated due to its potential for accelerating sampling and has sparked a range of works on specialized solvers for diffusion ODE [21, 22, 42]. Let Ψ denote an ODE solver, e.g., the deterministic diffusion implicit model (DDIM) solver [43]. The sampling iterates by:

$$x_{t_{n-1}} = \Psi(\epsilon_\theta(x_{t_n}, t_n), t_n, t_{n-1}), \quad (3)$$

where $\{t_n\}_{n=0}^N$ denotes a set of pre-defined discretization timesteps and $t_N = T, t_0 = 0$.

Latent diffusion models (LDMs) [32, 34] extend DMs to high-resolution image generation by converting pixel-level images into latent-space representations with an encoder E and a decoder D . Typically, E and D are jointly pre-trained under the variational auto-encoding principle [11].

2.2 Consistency Models

Consistency model (CM) [44, 45] aims at generating images from Gaussian noise within one sampling step. Its core idea is to learn a model $f_\theta(x_t, t)$ that directly maps any point x_t on the trajectory of the diffusion ODE to its endpoint. To achieve this, CMs first parameterizes $f_\theta(x_t, t)$ as:

$$f_\theta(x_t, t) = c_{skip}(t)x_t + c_{out}(t)F_\theta(x_t, t), \quad (4)$$

where $c_{skip}(t), c_{out}(t)$ is pre-defined to guarantee the boundary condition $f_\theta(x_0, 0) = x_0$, and $F_\theta(x_t, t)$ is the neural network (NN) to train.

CM can be learned from a pre-trained DM ϵ_{θ_0} via consistency distillation (CD) by minimizing [45]:

$$\mathcal{L}_{CD} = d(f_\theta(x_{t_m}, t_m), f_{\theta^-}(x_{t_n}, t_n)), \quad (5)$$

where $t_m \sim \mathcal{U}[0, T]$, $x_{t_m} \sim p_{t_m}(x_{t_m})$, $t_n \sim \mathcal{U}[0, t_m]$, $x_{t_n} = \Psi(\epsilon_{\theta_0}(x_{t_m}, t_m), t_m, t_n)$, $d(\cdot, \cdot)$ is some distance function, and θ^- is the exponential moving average (EMA) of θ . Typically, the solver Ψ only runs for one step for efficiency. Motivated by the success of CMs, latent CMs (LCMs) [23] apply latent consistency distillation (LCD) to LDMs for efficient high-resolution image synthesis, but suffer from degraded generations in practice.

2.3 Multistep Consistency Models

CMs learn the mapping between an arbitrary state of the entire ODE trajectory to the endpoint, which can cause significant learning difficulties and hence compromise generations [10]. To address this, multistep consistency models (MCMs) [4] generalize CMs by splitting the entire range $[0, T]$ into multiple segments and performing consistency distillation individually within each segment. Formally, MCMs first define a set of milestones $\{t_{\text{step}}^s\}_{s=0}^K$ (K denotes the number of segments), and minimize the following multistep consistency distillation (MCD) loss:

$$\mathcal{L}_{MCD} = d(\text{DDIM}(x_{t_m}, f_\theta(x_{t_m}, t_m), t_m, t_{\text{step}}^s), \text{DDIM}(x_{t_n}, f_{\theta-}(x_{t_n}, t_n), t_n, t_{\text{step}}^s)), \quad (6)$$

where s is uniformly sampled from $\{0, \dots, K\}$, $t_m \sim \mathcal{U}[t_{\text{step}}^s, t_{\text{step}}^{s+1}]$, $t_n \sim \mathcal{U}[t_{\text{step}}^s, t_m)$, and $\text{DDIM}(x_{t_m}, f_\theta(x_{t_m}, t_m), t_m, t_{\text{step}}^s)$ means one-step DDIM transformation from state x_{t_m} at timestep t_m to timestep t_{step}^s based on the estimated clean image $f_\theta(x_{t_m}, t_m)$ [42].

By simplifying the optimization problem, MCMs enjoy better convergence and higher generation quality. Besides, MCMs can naturally embrace multistep generation [4]. However, it is unclear if the MCM strategy can apply to large-scale LDMs and cope with the typical text-to-image generation. Our work aims at bridging this gap.

3 Methodology

Existing distillation-based acceleration approaches for LDMs either (i) depend on multiple individual distilled models for different sampling budgets [17, 28, 36], or (ii) sacrifice generation quality with limited (e.g., 2-4) and/or moderate (e.g., 5-8) sampling steps [20, 23, 33, 37, 38, 53]. We address these by incorporating the promising MCD strategy into LDMs. Besides, there are three technical contributions in the proposed Multistep Latent Consistency Models (MLCMs): 1) we extend MCD to embrace classifier-guidance (CFG) [7] strategy and develop a progressive training strategy to ensure inter-segment consistency. 2) We propose denoising consistency distillation which removes the reliance on training images and avoids the disparity between the training and inference of the model. 3) We incorporate reward learning techniques into MLCMs to further enhance human preference.

3.1 Multistep Latent Consistency Models

We consider distilling representative pre-trained LDMs, e.g., SDXL [32]. Let z_t denote the states at timestep t in the latent space. We abuse $\epsilon_{\theta_0}(z_t, c, t)$ and $f_\theta(z_t, c, t)$ to denote the pre-trained LDM and target model respectively, where c refers to the generation condition. We formulate the multistep latent consistency distillation (MLCD) loss for MLCMs as:

$$\mathcal{L}_{MLCD} = \|\text{DDIM}(z_{t_m}, f_\theta(z_{t_m}, c, t_m), t_m, t_{\text{step}}^s) - \text{nograd}(\text{DDIM}(z_{t_n}, f_\theta(z_{t_n}, c, t_n), t_n, t_{\text{step}}^s))\|_2^2, \quad (7)$$

where we make some specifications to Equation (6): 1) Instantiate the distance measure d as the L^2 distance for simplicity. 2) Replace the EMA model with a stop-gradient variant of the current model to minimize memory cost during training. 3) Fix $t_n = t_m - k$ with k as a skipping interval, which, unless specified otherwise, is set to 20 to balance convergence speed and generation quality.

Given CFG [7] is critical for high-quality text-to-image generation, we integrate it to MLCM by:

$$z_{t_n} = \Psi(\hat{\epsilon}_{\theta_0}(z_{t_m}, c, w, t_m), t_m, t_n), \quad (8)$$

where $\hat{\epsilon}_{\theta_0}(z_t, c, w, t) := \epsilon_{\theta_0}(z_t, \emptyset, t) + w(\epsilon_{\theta_0}(z_t, c, t) - \epsilon_{\theta_0}(z_t, \emptyset, t))$ with w as the guidance scale.

Better teacher brings further benefits. We empirically notice that the generation quality of MLCM can be further boosted by incorporating a better teacher ϵ_{θ_0} for estimating the ODE trajectory. In this sense, we advocate employing protovision-xl-v6.6 (PVXL) [49], a variant of SDXL fine-tuned on high-quality images, as ϵ_{θ_0} while remaining the model f_θ initialized from SDXL for improved results. Other strategies for a better estimation of the teacher trajectory [19] are left as future work.

3.2 Progressive MLCD

After a round of distillation on the K segments, MLCMs can naturally produce high-quality samples through K -step sampling. However, it is empirically observed that the performance decreases when

using fewer steps, shown in Appendix A.4, which is probably because of the larger discretization error caused by longer sampling step sizes. To alleviate this, we advocate explicitly teaching MLCMs to capture the mapping between the states that cross segments. This implies a progressive training procedure, where the gap between the timesteps t_m and t_n increases continually. Given this, we opt to use the MLCM trained in the previous stage, instead of the original pre-trained model, as the teacher to more precisely estimate z_{t_n} in only one solving step for distillation. This differentiates MLCM from HyperSD [33] which uses a fixed teacher. In practice, we reduce K by half in each new distillation stage and multiply the skipping interval k by 2 accordingly.

3.3 Image-free MCD with Samples from the Teacher

A common issue of the noise schedulers of LDMs is that the final noisy state z_T is not pure noise. For example, in SDXL, there is: $z_T = 0.068265z_0 + 0.99767\epsilon$ [25]. As a result, there exists a discrepancy between the training and inference of such DMs and the models that are distilled from them. We argue such a discrepancy can cause performance degradation during inference, especially when the sampling steps are few [16].

Inspired by the success of Imagine Flash [13], we propose to draw samples from the teacher models as training data to address this issue. This also helps to relieve the requirements for extensive high-quality text-image pairs. Specifically, instead of obtaining z_{t_m} via adding noise to z_0 as in MCM and HyperSD, we initialize z_T as pure Gaussian noise and perform denoising with off-the-shelf ODE solvers based on the teacher model ϵ_{θ_0} to obtain z_{t_m} . Intuitively, with this strategy, we leverage and distill only the denoising ODE trajectory of the teacher without concerning the forward one.

The latent state z_{t_m} can be acquired by one-step sampling, but we empirically find this naive strategy is unable to enhance the performance of MLCD. This is because this method easily generates blurry and semantically inconsistent samples. Theoretically, z_{t_m} contains less noise for smaller t_m . Therefore, we design a multistep denoising strategy (MDS) to predict z_{t_m} , which executes more iterations for smaller t_m to get cleaner z_{t_m} . For the first stage of MLCD to calculate z_{t_m} , we present the details in Algorithm 1 in the appendix A.3. For the progressive training stage, the procedure to compute z_{t_m} is described in Algorithm 2 in the appendix A.3. Figure 2 illustrates image-free MLCD in the first stage and progressive stage, where we take initial segment number $K = 4$ as an example. In the first stage, DDIM sampler is used to estimate ODE trajectory and calculate from pure Gaussian noise. Based on the previous MLCD results, image-free progressive training is used to enforce consistency on the states that cross previous segments with reduced segment number, where the trained MLCM is used to estimate trajectory and z_{t_m} .

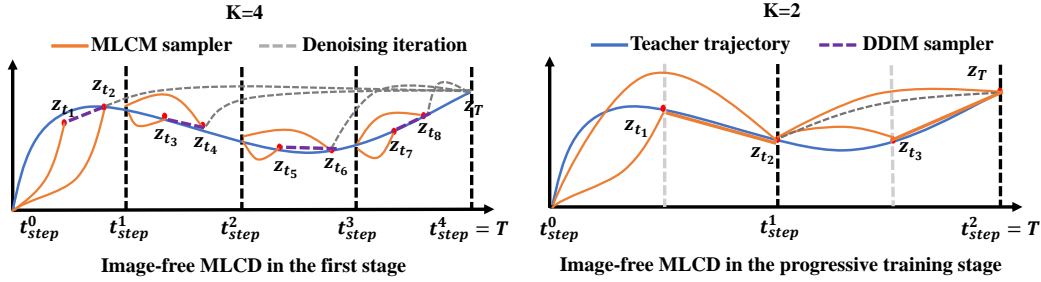


Figure 2: An illustration of the image-free MLCD in the first stage and progressive stage. The first stage divides the entire timestep range $[0, T]$ into $K = 4$ segments. Segment-wise LCD is performed within each segment $[t_{step}^s, t_{step}^{s+1}]$ by mapping each point to $z_{t_{step}^s}$. The latent codes z_{t_m} , e.g., z_{t_8} , z_{t_6} , are calculated by denoising pure Gaussian noise z_T with one-step and two-step DDIM sampler. In the progressive stage, the segment number decreases by half. The trained MLCM is used to compute z_{t_m} and the teacher trajectory.

3.4 Reward Consistency and Feedback Learning

Barely relying on the L^2 loss in Equation (7) for distillation makes the distilled model unaware of human preference. To bridge the gap, we propose to incorporate human preference scorers $s(x, c)$,

e.g., IR [52] and AS [39], to define extra regularization for improving the visual quality. Specifically, we define the following reward consistency loss, where the latent codes are projected back to pixel space and a consistent score of them is demanded:

$$\mathcal{L}_{RC} = \|s(D(\text{DDIM}(z_{t_m}, f_{\theta}(z_{t_m}, c, t_m), t_m, t_{\text{step}}^s)), c) - s(D(\text{nograd}(\text{DDIM}(z_{t_n}, f_{\theta}(z_{t_n}, c, t_n), t_n, t_{\text{step}}^s))), c)\|_2^2. \quad (9)$$

Given that in the late stages of training, MLCMs can generate realistic samples \hat{x}_0 in one or two steps, we can naturally directly maximize the feedback of the scorer on the sample $s(\hat{x}_0, c)$. Formally, we optimize the following hinge loss with a margin s_0 :

$$\mathcal{L}_{FL} = \max(s_0 - s(x_0, c), 0). \quad (10)$$

The gradients are directly back-propagated from the scorer to model parameters θ for optimization.

Table 1: Quantitative comparisons on MSCOCO-2017 5K validation datasets. All models adopts SDXL architecture.

Method	Step	CS	AS	IR	PS
DDIM [42]	25	33.36	5.54	0.87	0.229
LCM [23]	4	32.53	5.42	0.48	0.224
SDXL-Turbo [38]	4	33.30	5.64	0.83	0.226
SDXL-Lightning [17]	4	32.40	5.63	0.72	0.229
SDXL-Lightning [17]	8	32.73	5.95	0.71	0.227
HyperSD [33]	4	32.64	5.52	1.15	0.234
HyperSD [33]	8	32.41	5.83	1.14	0.233
MLCM	2	33.02	6.10	1.10	0.227
MLCM	3	33.24	6.17	1.18	0.232
MLCM	4	33.30	6.19	1.20	0.233
MLCM	8	33.48	6.20	1.22	0.233

4 Experiments

4.1 Main Results

We quantitatively compare our method with both the DDIM [42] baseline and acceleration approaches including LCM [23], SDXL-Turbo [38], SDXL-Lightning [17], HyperSD [33]. CS [5] with ViT-g/14 backbone, AS [39], IR [52], PS [12], are exploited as objective metrics. The evaluation is performed on MSCOCO-2017 5K validation dataset [18]. All methods perform zero-shot validation except for HyperSD since it utilizes the MSCOCO-2017 dataset for training.

The metrics of various methods are listed in Table 1. Among all the methods, our 2-step MLCM presents superior CS, AS, IR, and PS than 4-step LCM [23], 8-step SDXL-Lightning [17], 8-step HyperSD [33]. These results indicate our MLCM’s synthetic images are better aligned with texts and the human preference than LCM, SDXL-Lightning. Although 2-MLCM shows slightly lower CS than 4-step SDXL-Turbo, 2-MLCM enjoys much higher AS, IR, and PS. Compared to 8-step HyperSD, 4-step MLCM obtains large improvements in terms of CS, AS, IR, and comparable PS, although HyperSD uses MSCOCO for training, which validates that our method is more powerful to generate high-quality images with few-step inference. Moreover, We can observe from Table 1 that our MLCM can improve the quality of the generated images with additional steps.

We present the visual comparisons in Figure 3. Under the same conditions, we observe that the images generated by MLCM have backgrounds with more intricate details and maintain higher semantic consistency on more challenging prompts, which also leads to greater human preference. Besides, MLCM can be leveraged as a plug-and-play module to provide acceleration capabilities for other tasks, e.g. controllable generation. We provide some examples generated by ControlNet [56] with MLCM for illustration in Figure 4. We include several illustrative examples using MLCM on tasks like image style transfer in Appendix A.2.1 and Chinese-to-image in Appendix A.2.2 to demonstrate the generality of MLCM.

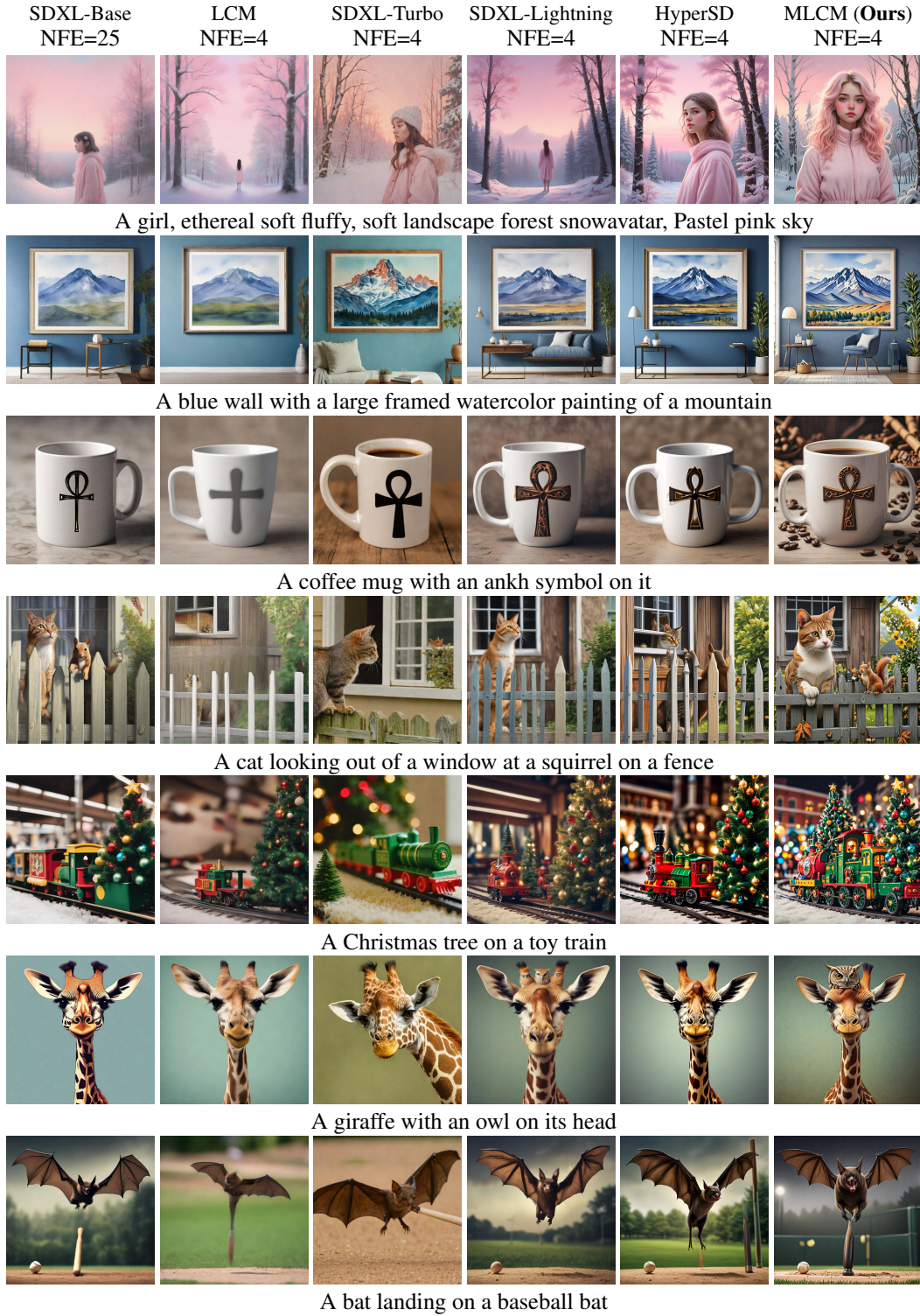


Figure 3: Visual comparison between our MLCM and baseline methods. The prompts are basically from Parti-Prompts [55]. We can observe that our MLCM can exhibit a richness in detail (the first three rows) and better semantic coherence (the latter four rows), leading to better alignment with human preference. Zoom in for more details.



Figure 4: MLCM with ControlNet. Our MLCM can be incorporated into ControlNet pipeline and produce satisfactory results with 2 steps sampling.

Table 2: Ablation study of MLCM with respect to MLCD, single denoising iteration (SDI), multistep denoising iterations (MDI), reward consistency (RC), feedback learning (FL), progressive distillation with fixed teacher (PDF), progressive distillation with updated teacher (PDU). LCD (SDXL) represents the teacher is SDXL during LCD, otherwise, the teacher is PVXL.

Method	Step	CS	AS	IR	PS
LCD (SDXL)	4	32.53	5.42	0.48	0.224
MLCD (SDXL)	4	32.74	5.88	0.92	0.224
MLCD	4	32.68	6.01	0.94	0.225
MLCD+ SDI	4	32.67	5.96	0.91	0.224
MLCD+ MDI	4	33.00	6.03	0.95	0.225
MLCD+ MDI+ RC	4	33.08	6.06	0.97	0.225
MLCD+ MDI+ RC+ PDF	4	33.22	6.07	0.97	0.225
MLCD+ MDI+ RC+ PDU	4	33.28	6.10	1.05	0.230
MLCM (SDXL)	4	33.02	6.17	1.15	0.232
MLCM	4	33.30	6.19	1.20	0.233

4.2 Ablation Study

To analyze the key components of our method, we make a thorough ablation study to verify the effectiveness of the proposed MLCM. Table 2 depicts the performance of MLCM’s variants. All the models use PVXL as the initial teacher except where specified to use SDXL instead.

Multistep latent consistency distillation. It can be seen from Table 2 that MLCD (SDXL) outperforms LCD (SDXL) by a large margin, which verifies that MLCD has a stronger capability to accelerate LDM than LCD. This is because it is hard for LCD to enforce consistency across the entire timestep range while MLCD alleviates this by performing latent consistency distillation within each segment.

Image-free MLCD. As outlined in Table 2, MLCD + SDI achieves comparable performance to MLCD, indicating our denoising MLCD is capable of training MLCM without requiring any training images. The performance is substantially enhanced by substituting SDI with MDI in terms of CS, AS, IR, verifying that the proposed multistep denoising iterations is critical to optimize MLCM.

Reward consistency. As depicted in Table 2, the CS, AS, and IR values are improved by adding RC to MLCD+ MDI, demonstrating the effectiveness of the reward consistency.

Progressive MLCD. We can observe that both PDF and PDU introduce gains to MLCD+ MDI+ RC, especially for CS value. This is because progressive MLCD reduces segment number and further boosts segment-wise consistency along pre-defined points at the inference stage. Furthermore, Table 2

demonstrates that using trained MLCM in the previous stage significantly surpasses the fixed raw teacher with respect to human preference metrics. The reason behind this is the trained MLCM is much more powerful in predicting consistency trajectory for large skipping time steps.

Feedback learning. As shown in Table 2, our MLCM obtains remarkable improvements over MLCD+ MDI+ RC+ PD on all metrics via the proposed feedback learning, because it steers MLCM toward the higher human preference generation.

Teacher trajectory. As listed in Table 1, using different teacher models to estimate the trajectory can influence the performance of MLCM. MLCM achieves better performance than MLCM (SDXL) using SDXL as the teacher since PVXL provides a more accurate trajectory in MLCD. Also, we can observe from Table 1 and Table 2 that our 4-step MLCM (SDXL) again significantly outperforms 4-step LCM, 8-step SDXL-Lightning, in terms of CS, AS, IR. Meanwhile, 4-step MLCM (SDXL) shows much higher CS and AS values than 8-step HyperSD, keeping comparable IR and PS values. These results demonstrate the superiority of this method over other works on accelerating LDMs.

5 Related works

Diffusion models (DMs) [6, 41, 46, 47, 48] progressively add Gaussian noise to perturb the data, then are trained to denoise noise-corrupted data. In the inference stage, DMs sample from a Gaussian distribution and perform sequential denoising steps to reconstruct the data. As a type of generative model, they have demonstrated impressive capabilities in generating realistic and high-quality outputs in text-to-image generation [32, 34, 35], video generation [31], and audio generation [14]. To enhance the condition awareness in conditional DMs, the classifier-free guidance (CFG) [7] technique is proposed to trade off diversity and fidelity.

Diffusion acceleration. The primary challenges that hinder the practical adoption of DMs is the slow inference involving tens to hundreds of evaluations of the model. Early works like Progressive Distillation (PD) [36] and Classifier-aware Distillation (CAD) [28] explore the approaches of progressive knowledge distillation to compress sampling steps but lead to blurry samples within four sampling steps. Consistency models (CMs) [45], consistency trajectory models (CTMs) [10] and Diff-Instruct [24] distill a pre-trained DM into a single-step generator, but they do not verify the effectiveness on large-scale text-to-image generation.

Recently, the distillation of large-scale text-to-image DMs has gained significant attention. LCM [23] extends CM to text-to-image generation with few-step inference but synthesizes blurry images in four steps. InstaFlow [20], UFOGen [53], SwiftBrush [30] and DMD [54] propose one-step sampling for text-to-image generation but are unable to extend their sampler to multiple steps for better image quality. More recently, SDXL-Turbo [38], SDXL-Lighting [17] and HyperSD [33] are proposed to further enhance the image quality with few-step sampling but their training depends on huge high-quality text-image pairs. Our method not only enables the generation of high-quality samples using a 2-4 steps sampler but also enhances model performance as the number of steps increases. Furthermore, our training strategy is resource-efficient and does not require any images.

Feedback learning. While text-to-image DMs are capable of generating plausible images in the majority of cases, they still suffer from inferior visual generation quality and misalignment with human aesthetic preferences. Supervised Learning [15, 51], RLHF-based [1, 3] and DPO-based [50] are popular for better image quality. Among the various fine-tuning methods proposed, reward feedback learning (ReFL) [2, 52] stands out as a widely used approach that calculates the gradient of rewards. In our framework, we can leverage few-step generations of MLCMs to directly guide model tuning, improving the performance of MLCM without raising significant computation overheads.

6 Conclusion & Limitation

In this paper, we propose Multistep Latent Consistency Model (MLCM), a novel approach for accelerating text-to-image latent diffusion models without requiring any text-image paired data. MLCM can generate high-quality, delightful images with only 2-8 sampling steps and achieve better image quality than baseline methods while being compatible with controllable generation, image style transfer, and Chinese-to-image generation.

Limitation. In our experiments, we observe that MLCM still has room for improvement in single-step generation, which we plan to focus on in our future work.

References

- [1] Kevin Black, Michael Janner, Yilun Du, Ilya Kostrikov, and Sergey Levine. Training diffusion models with reinforcement learning. *arXiv preprint arXiv:2305.13301*, 2023.
- [2] Kevin Clark, Paul Vicol, Kevin Swersky, and David J Fleet. Directly fine-tuning diffusion models on differentiable rewards. In *The Twelfth International Conference on Learning Representations*, 2023.
- [3] Ying Fan, Olivia Watkins, Yuqing Du, Hao Liu, Moonkyung Ryu, Craig Boutilier, Pieter Abbeel, Mohammad Ghavamzadeh, Kangwook Lee, and Kimin Lee. Reinforcement learning for fine-tuning text-to-image diffusion models. *Advances in Neural Information Processing Systems*, 36, 2024.
- [4] Jonathan Heek, Emiel Hoogeboom, and Tim Salimans. Multistep consistency models. *arXiv preprint arXiv:2403.06807*, 2024.
- [5] Jack Hessel, Ari Holtzman, Maxwell Forbes, Ronan Le Bras, and Yejin Choi. CLIPScore: a reference-free evaluation metric for image captioning. In *EMNLP*, 2021.
- [6] Jonathan Ho, Ajay Jain, and Pieter Abbeel. Denoising diffusion probabilistic models. *Advances in neural information processing systems*, 33:6840–6851, 2020.
- [7] Jonathan Ho and Tim Salimans. Classifier-free diffusion guidance. *arXiv preprint arXiv:2207.12598*, 2022.
- [8] Edward J Hu, Phillip Wallis, Zeyuan Allen-Zhu, Yuanzhi Li, Shean Wang, Lu Wang, Weizhu Chen, et al. Lora: Low-rank adaptation of large language models. In *International Conference on Learning Representations*, 2021.
- [9] Tero Karras, Miika Aittala, Timo Aila, and Samuli Laine. Elucidating the design space of diffusion-based generative models. *Advances in Neural Information Processing Systems*, 35:26565–26577, 2022.
- [10] Dongjun Kim, Chieh-Hsin Lai, Wei-Hsiang Liao, Naoki Murata, Yuhta Takida, Toshimitsu Uesaka, Yutong He, Yuki Mitsufuji, and Stefano Ermon. Consistency trajectory models: Learning probability flow ode trajectory of diffusion. *arXiv preprint arXiv:2310.02279*, 2023.
- [11] Diederik P Kingma and Max Welling. Auto-encoding variational bayes. *stat*, 1050:1, 2014.
- [12] Yuval Kirstain, Adam Polyak, Uriel Singer, Shahbuland Matiana, Joe Penna, and Omer Levy. Pick-a-pic: An open dataset of user preferences for text-to-image generation. *Advances in Neural Information Processing Systems*, 36, 2024.
- [13] Jonas Kohler, Albert Pumarola, Edgar Schönfeld, Artsiom Sanakoyeu, Roshan Sumbaly, Peter Vajda, and Ali Thabet. Imagine flash: Accelerating emu diffusion models with backward distillation. *arXiv preprint arXiv:2405.05224*, 2024.
- [14] Zhifeng Kong, Wei Ping, Jiaji Huang, Kexin Zhao, and Bryan Catanzaro. Diffwave: A versatile diffusion model for audio synthesis. *arXiv preprint arXiv:2009.09761*, 2020.
- [15] Kimin Lee, Hao Liu, Moonkyung Ryu, Olivia Watkins, Yuqing Du, Craig Boutilier, Pieter Abbeel, Mohammad Ghavamzadeh, and Shixiang Shane Gu. Aligning text-to-image models using human feedback. *arXiv preprint arXiv:2302.12192*, 2023.
- [16] Shanchuan Lin, Bingchen Liu, Jiashi Li, and Xiao Yang. Common diffusion noise schedules and sample steps are flawed. In *Proceedings of the IEEE/CVF Winter Conference on Applications of Computer Vision*, pages 5404–5411, 2024.
- [17] Shanchuan Lin, Anran Wang, and Xiao Yang. Sdxl-lightning: Progressive adversarial diffusion distillation. *arXiv preprint arXiv:2402.13929*, 2024.
- [18] Tsung-Yi Lin, Michael Maire, Serge Belongie, James Hays, Pietro Perona, Deva Ramanan, Piotr Dollár, and C Lawrence Zitnick. Microsoft coco: Common objects in context. In *Computer Vision—ECCV 2014: 13th European Conference, Zurich, Switzerland, September 6-12, 2014, Proceedings, Part V 13*, pages 740–755. Springer, 2014.
- [19] Hongjian Liu, Qingsong Xie, Zhijie Deng, Chen Chen, Shixiang Tang, Fueyang Fu, Zhengjun Zha, and Haonan Lu. Scott: Accelerating diffusion models with stochastic consistency distillation. *arXiv preprint arXiv:2403.01505*, 2024.

- [20] Xingchao Liu, Xiwen Zhang, Jianzhu Ma, Jian Peng, and Qiang Liu. Instaflo: One step is enough for high-quality diffusion-based text-to-image generation. *arXiv preprint arXiv:2309.06380*, 2023.
- [21] Cheng Lu, Yuhao Zhou, Fan Bao, Jianfei Chen, Chongxuan Li, and Jun Zhu. Dpm-solver: A fast ode solver for diffusion probabilistic model sampling in around 10 steps. *Advances in Neural Information Processing Systems*, 35:5775–5787, 2022.
- [22] Cheng Lu, Yuhao Zhou, Fan Bao, Jianfei Chen, Chongxuan Li, and Jun Zhu. Dpm-solver++: Fast solver for guided sampling of diffusion probabilistic models. *arXiv preprint arXiv:2211.01095*, 2022.
- [23] Simian Luo, Yiqin Tan, Longbo Huang, Jian Li, and Hang Zhao. Latent consistency models: Synthesizing high-resolution images with few-step inference. *arXiv preprint arXiv:2310.04378*, 2023.
- [24] Weijian Luo, Tianyang Hu, Shifeng Zhang, Jiacheng Sun, Zhenguo Li, and Zhihua Zhang. Diff-instruct: A universal approach for transferring knowledge from pre-trained diffusion models. *arXiv preprint arXiv:2305.18455*, 2023.
- [25] Yihong Luo, Xiaolong Chen, and Jing Tang. You only sample once: Taming one-step text-to-image synthesis by self-cooperative diffusion gans. *arXiv preprint arXiv:2403.12931*, 2024.
- [26] Jian Ma, Chen Chen, Qingsong Xie, and Haonan Lu. Pea-diffusion: Parameter-efficient adapter with knowledge distillation in non-english text-to-image generation. *arXiv preprint arXiv:2311.17086*, 2023.
- [27] Xin Ma, Yaohui Wang, Gengyun Jia, Xinyuan Chen, Ziwei Liu, Yuan-Fang Li, Cunjian Chen, and Yu Qiao. Latte: Latent diffusion transformer for video generation. *arXiv preprint arXiv:2401.03048*, 2024.
- [28] Chenlin Meng, Robin Rombach, Ruiqi Gao, Diederik Kingma, Stefano Ermon, Jonathan Ho, and Tim Salimans. On distillation of guided diffusion models. In *Proceedings of the IEEE/CVF Conference on Computer Vision and Pattern Recognition*, pages 14297–14306, 2023.
- [29] Chong Mou, Xintao Wang, Liangbin Xie, Yanze Wu, Jian Zhang, Zhongang Qi, and Ying Shan. T2i-adapter: Learning adapters to dig out more controllable ability for text-to-image diffusion models. In *Proceedings of the AAAI Conference on Artificial Intelligence*, volume 38, pages 4296–4304, 2024.
- [30] Thuan Hoang Nguyen and Anh Tran. Swiftbrush: One-step text-to-image diffusion model with variational score distillation. *arXiv preprint arXiv:2312.05239*, 2023.
- [31] William Peebles and Saining Xie. Scalable diffusion models with transformers. In *Proceedings of the IEEE/CVF International Conference on Computer Vision*, pages 4195–4205, 2023.
- [32] Dustin Podell, Zion English, Kyle Lacey, Andreas Blattmann, Tim Dockhorn, Jonas Müller, Joe Penna, and Robin Rombach. Sdxl: Improving latent diffusion models for high-resolution image synthesis. In *The Twelfth International Conference on Learning Representations*, 2023.
- [33] Yuxi Ren, Xin Xia, Yanzuo Lu, Jiacheng Zhang, Jie Wu, Pan Xie, Xing Wang, and Xuefeng Xiao. Hyper-sd: Trajectory segmented consistency model for efficient image synthesis. *arXiv preprint arXiv:2404.13686*, 2024.
- [34] Robin Rombach, Andreas Blattmann, Dominik Lorenz, Patrick Esser, and Björn Ommer. High-resolution image synthesis with latent diffusion models. In *Proceedings of the IEEE/CVF conference on computer vision and pattern recognition*, pages 10684–10695, 2022.
- [35] Chitwan Saharia, William Chan, Saurabh Saxena, Lala Li, Jay Whang, Emily L Denton, Kamyar Ghasemipour, Raphael Gontijo Lopes, Burcu Karagol Ayan, Tim Salimans, et al. Photorealistic text-to-image diffusion models with deep language understanding. *Advances in neural information processing systems*, 35:36479–36494, 2022.
- [36] Tim Salimans and Jonathan Ho. Progressive distillation for fast sampling of diffusion models. In *International Conference on Learning Representations*, 2022.
- [37] Axel Sauer, Frederic Boesel, Tim Dockhorn, Andreas Blattmann, Patrick Esser, and Robin Rombach. Fast high-resolution image synthesis with latent adversarial diffusion distillation. *arXiv preprint arXiv:2403.12015*, 2024.

- [38] Axel Sauer, Dominik Lorenz, Andreas Blattmann, and Robin Rombach. Adversarial diffusion distillation. *arXiv preprint arXiv:2311.17042*, 2023.
- [39] Christoph Schuhmann. Clip+mlp aesthetic score predictor. <https://github.com/christophschuhmann/improved-aesthetic-predictor>. Accessed: 2024-05-20.
- [40] Christoph Schuhmann, Romain Beaumont, Richard Vencu, Cade Gordon, Ross Wightman, Mehdi Cherti, Theo Coombes, Aarush Katta, Clayton Mullis, Mitchell Wortsman, et al. Laion-5b: An open large-scale dataset for training next generation image-text models. *Advances in Neural Information Processing Systems*, 35:25278–25294, 2022.
- [41] Jascha Sohl-Dickstein, Eric Weiss, Niru Maheswaranathan, and Surya Ganguli. Deep unsupervised learning using nonequilibrium thermodynamics. In *International conference on machine learning*, pages 2256–2265. PMLR, 2015.
- [42] Jiaming Song, Chenlin Meng, and Stefano Ermon. Denoising diffusion implicit models. In *International Conference on Learning Representations*, 2020.
- [43] Jiaming Song, Chenlin Meng, and Stefano Ermon. Denoising diffusion implicit models. *arXiv preprint arXiv:2010.02502*, 2020.
- [44] Yang Song and Prafulla Dhariwal. Improved techniques for training consistency models. *arXiv preprint arXiv:2310.14189*, 2023.
- [45] Yang Song, Prafulla Dhariwal, Mark Chen, and Ilya Sutskever. Consistency models. *arXiv preprint arXiv:2303.01469*, 2023.
- [46] Yang Song and Stefano Ermon. Generative modeling by estimating gradients of the data distribution. *Advances in neural information processing systems*, 32, 2019.
- [47] Yang Song and Stefano Ermon. Improved techniques for training score-based generative models. *Advances in neural information processing systems*, 33:12438–12448, 2020.
- [48] Yang Song, Jascha Sohl-Dickstein, Diederik P Kingma, Abhishek Kumar, Stefano Ermon, and Ben Poole. Score-based generative modeling through stochastic differential equations. In *International Conference on Learning Representations*, 2020.
- [49] stablediffusionapi. protovision-xl-v6.6. <https://huggingface.co/stablediffusionapi/protovision-xl-v6.6>. Accessed: 2024-05-20.
- [50] Bram Wallace, Meihua Dang, Rafael Rafailov, Linqi Zhou, Aaron Lou, Senthil Purushwalkam, Stefano Ermon, Caiming Xiong, Shafiq Joty, and Nikhil Naik. Diffusion model alignment using direct preference optimization. *arXiv preprint arXiv:2311.12908*, 2023.
- [51] Xiaoshi Wu, Keqiang Sun, Feng Zhu, Rui Zhao, and Hongsheng Li. Better aligning text-to-image models with human preference. *arXiv preprint arXiv:2303.14420*, 2023.
- [52] Jiazheng Xu, Xiao Liu, Yuchen Wu, Yuxuan Tong, Qinkai Li, Ming Ding, Jie Tang, and Yuxiao Dong. Imagereward: Learning and evaluating human preferences for text-to-image generation. *Advances in Neural Information Processing Systems*, 36, 2024.
- [53] Yanwu Xu, Yang Zhao, Zhisheng Xiao, and Tingbo Hou. Ufogen: You forward once large scale text-to-image generation via diffusion gans. *arXiv preprint arXiv:2311.09257*, 2023.
- [54] Tianwei Yin, Michaël Gharbi, Richard Zhang, Eli Shechtman, Fredo Durand, William T Freeman, and Taesung Park. One-step diffusion with distribution matching distillation. *arXiv preprint arXiv:2311.18828*, 2023.
- [55] Jiahui Yu, Yuanzhong Xu, Jing Yu Koh, Thang Luong, Gunjan Baid, Zirui Wang, Vijay Vasudevan, Alexander Ku, et al. Scaling autoregressive models for content-rich text-to-image generation. *arXiv preprint arXiv:2206.10789*, 2(3):5, 2022.
- [56] Lvmin Zhang, Anyi Rao, and Maneesh Agrawala. Adding conditional control to text-to-image diffusion models. In *Proceedings of the IEEE/CVF International Conference on Computer Vision*, pages 3836–3847, 2023.

A Appendix / supplemental material

A.1 Implementation Details

We use the prompts from LAION-Aesthetics- 6+ subset of LAION-5B [40] to train our model. We train the model with 4 A100 and a batch size of 24 for 40,000 iterations. The learning rate is 1e-5 with Adam optimizer. The initial segment number K is 8 and s_0 for IR and AS are 2.0 and 8.0, respectively. The total loss function to train MLCM is:

$$\mathcal{L} = \mathcal{L}_{MLCD} + \mathcal{L}_{RC} + w_{FL}\mathcal{L}_{FL}, \quad (11)$$

where w_{FL} is 1e-3. We set the guidance scale w in CFG as 8.0. As for model configuration, we use PVXL [49] as the default teacher to estimate trajectory while student model f_θ is initialized by SDXL [17]. We also conduct the experiment adopting SDXL as a teacher for fair comparisons with other methods. We train a unified Lora instead of UNet in all the distillation stages for convenient transfer to downstream applications.

A.2 Application

A.2.1 Acceleration of Image Style Transfer

Our MLCM LoRA is compatible with the pipeline of image style transfer [29]. We present some examples in Figure 5 with only 2-step sampling.

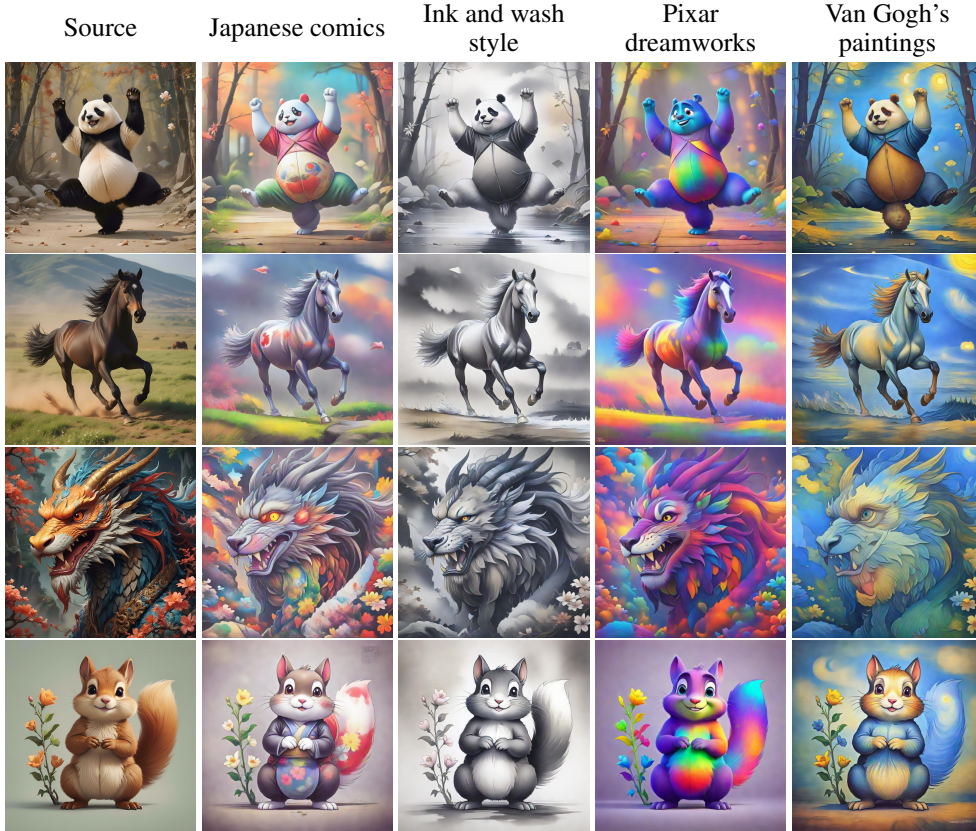


Figure 5: MLCM with image style transfer. The styles are presented at the top, and we apply image style transfer on the source image with our MLCM. Two-step sampling can produce highly stylized images with excellent results.



Figure 6: MLCM for Chinese-to-image generation. With 3 steps sampling, our MLCM model can produce images that align with Chinese semantic meaning. The first line presents images in general Chinese contexts, while the second line showcases images in specific Chinese cultural settings.

A.2.2 Acceleration of Chinese-to-image Generation

Our MLCM can accelerate the generation speed of Chinese-to-image diffusion model [26]. We present some examples in Figure 6.

A.3 Algorithms

Algorithm 1: Denoising iterations of teacher generating latent code in the first stage of MLCD

Input: Gaussian noise ϵ , timestep t_m , segment index s , teacher model ϵ_{θ_0} , text condition c , segment number K

Initialize z_T with ϵ , calculate denoising steps $L = K - s$, time interval $\Delta T = (T - t_m)/L$

for i **in** $\{0, 1, \dots, L - 1\}$ **do**
 Calculate $t = T - i * \Delta T$, $t_{m'} = t - \Delta T$
 Calculate $z_{t_{m'}} = \Psi(\hat{\epsilon}_{\theta_0}(z_t, c, w, t), t, t_{m'})$
end

Algorithm 2: Denoising iterations of MLCM to generate latent code in the progressive stage

Input: Gaussian noise ϵ , timestep t_m , MLCM f_{θ}^t , text condition c , segment number K

Initialize z_T with ϵ , calculate time interval $\Delta T = T/(2K)$ and denoising steps

$L = (T - t_m)/\Delta T$
for i **in** $\{0, 1, \dots, L - 1\}$ **do**
 Calculate $t = T - i * \Delta T$, $t_{m'} = t - \Delta T$
 Calculate $z_{t_{m'}} = \text{DDIM}(z_t, f_{\theta}^t(z_t, c, t), t, t_{m'})$
end

A.4 The first stage of training

After the first stage of training, the MLCM can generate clear images with K -step sampling. However, the results from sampling with fewer than K steps are still unsatisfactory. We provide some intermediate samples in Figure 7, which also demonstrate the importance of progressive training.

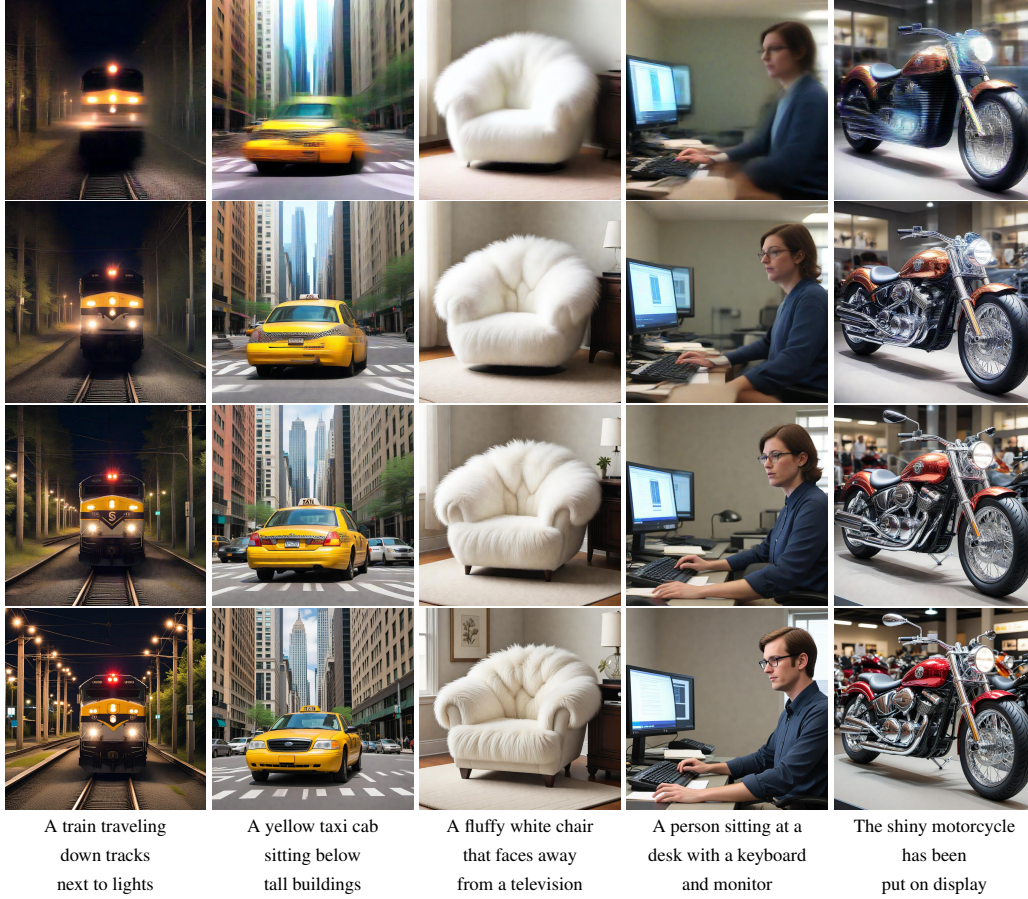


Figure 7: Examples after the first stage of MLCM training. From top to bottom, 2, 3, 4 and 8 sampling steps are adopted, respectively. We extract prompts from MSCOCO dataset but omit them for simplicity. We observe that 4-step sampling can achieve satisfactory results, while 2&3-step sampling still produces blurry images.

A.5 Broader Impact

Our work has the potential to lead to significant societal consequences. Similar to other generative models, DPMs could be utilized to create misleading or even harmful content. Furthermore, our method may exacerbate the negative impact of malicious uses of generative AI.